

This is an Open Access document downloaded from ORCA, Cardiff University's institutional repository: <https://orca.cardiff.ac.uk/id/eprint/145745/>

This is the author's version of a work that was submitted to / accepted for publication.

Citation for final published version:

Niland, Andrew, Santhosh, R., Marsh, Richard and Bowen, Philip 2022. Experimental investigation of effervescent atomization: Part I. Comparison of flat-end and streamlined aerator body designs. *Atomization and Sprays* 32 (4) , pp. 53-75. 10.1615/AtomizSpr.2022039407

Publishers page: <https://doi.org/10.1615/AtomizSpr.2022039407>

Please note:

Changes made as a result of publishing processes such as copy-editing, formatting and page numbers may not be reflected in this version. For the definitive version of this publication, please refer to the published source. You are advised to consult the publisher's version if you wish to cite this paper.

This version is being made available in accordance with publisher policies. See <http://orca.cf.ac.uk/policies.html> for usage policies. Copyright and moral rights for publications made available in ORCA are retained by the copyright holders.



Experimental investigation of effervescent atomization: Part I. Comparison of flat-end and streamlined aerator body designs

Andrew Niland^a, R. Santhosh^{b*}, Richard Marsh^a, Philip Bowen^{a*}

^aCardiff School of Engineering, Cardiff University, Wales CF24 3AA, UK

^bDepartment of Mechanical Engineering, Indian Institute of Technology (BHU) Varanasi,
Varanasi 221005, India

rsanthosh.mec@iitbhu.ac.in

bowenpj@cardiff.ac.uk

Abstract

The present experimental work is concerned with the study of effervescent atomisation, a two-phase gas-liquid spray generation technique that offers many advantages over conventional atomisers. This study shows the advantage of streamlined aerator design over flat-end aerator type with respect to formation of gas void in the aerator wake in the interior of an *inside-out* type of effervescent atomizer. The experiments are performed employing high-speed shadowgraphy visualizations. It is observed that in the conventional flat-end type of aerator design the formation of gas void is undesirable and leads to spray characterized by instabilities, causing fluctuating spray properties. The existence of gas void also prevents the formation of bubbly flow inside the effervescent atomizer which is actually preferred in these types of atomizers to enable stable spray generation and fine atomization. The formation and existence of gas void is found to be a result of aerator bluff body recirculation and gas phase buoyancy effects.

Four different streamlined aerator designs with tips in the shape of circular arc, circular arc/conical hybrid, conical and DARPA SUBOFF afterbody design (which is common in the conventional ship designs) are evaluated to determine the best among them with respect to mitigating the unwanted gas-void in the interior of an effervescent atomizer. These are evaluated with respect to ability to produce bubbly flow over comparatively large operating range and the ability to impart minimum wake (of aerator body) effect. It is concluded, upon careful experimental observations, that DARPA SUBOFF afterbody design is the best among the streamlined aerator designs.

Keywords: effervescent atomization, internal-flow visualization, gas-void, streamlined aerator body, bubbly flow, wake effect

Nomenclature

Roman Characters

Symbol	Definition	Unit
A_{MC}	Mixing chamber cross-sectional area	m^2
G_l	Liquid mass flux	$kg/m^2\cdot s$
G_g	Gas mass flux	$kg/m^2\cdot s$
\dot{m}_g	Gas mass flow rate	kg/s
\dot{m}_l	Liquid mass flow rate	kg/s
ϕm	diameter of aerator holes	-
n	no. of aerator holes	-

Greek Symbols

Symbol	Definition	Unit
σ	Surface tension	kg/s^2
ρ_g	Gas density, where ρ_a is air density	kg/m^3
ρ_l	Liquid density, where ρ_w is water density	kg/m^3
μ_l	Liquid dynamic viscosity, where μ_w is water dynamic viscosity	kg/ms
ν_l	Liquid kinematic viscosity, where ν_w is water kinematic viscosity	m^2/s
Ψ	$= \left(\frac{\sigma_l}{\sigma_w} \right)^{-1} \left(\frac{\rho_l}{\rho_w} \right)^{-2.3} \left(\frac{\mu_l}{\mu_w} \right)^{1.3}$;	-
λ	$= \sqrt{\left(\frac{\rho_g}{\rho_a} \right) \left(\frac{\rho_l}{\rho_w} \right)}$	-
$G_l \Psi$	Liquid Baker parameter	$kg/m^2\cdot s$
$\frac{G_g}{\lambda}$	Gas Baker parameter	$kg/m^2\cdot s$

Acronyms

Acronym	Definition
ADARPA	DARPA SUBOFF afterbody
ALR	Air-to-liquid mass ratio

Dimensionless Parameters

Parameter	Definition
Re	Reynolds number
We	Weber number
Oh	Ohnesorge number

1. Introduction

The effervescent atomisation, developed by Lefebvre and co-workers (Lefebvre et al., 1988; Lefebvre, 1988; Roesler and Lefebvre, 1989; Wang et al., 1989), involves injection of atomising gas at low velocity into a liquid flow through an aerator (Figure 1a) to form a two-phase bubbly mixture (in the mixing chamber). The two-phase flow is then forced through a narrow exit orifice (Figure 1a), where a substantial pressure drop occurs, causing the gas bubbles to burst and shatter the liquid core into droplets and ligaments. There are a number of advantages of effervescent atomisation compared to conventional atomisation methods. First, compared to a pressure atomiser the spray quality in effervescent atomisation is better at low operating pressures (Sovani et al, 2001; Lefebvre, 1989; Jedelsky et al., 2009), reducing operating costs and component wear, and, due to the larger exit orifices the likelihood of blockage is reduced (Lefebvre, 1988b; Sovani et al, 2001; Catlin et al., 2001; Jedelsky et al., 2009; Kim et al., 2001; Lörcher et al., 2005). Second, the effervescent atomisation is less sensitive to liquid properties, in particular, one atomiser can spray a range of liquids without much modification (Lefebvre, 1988; Jagannathan et al., 2011; Gosselin et al., 1994; Jedelsky et al., 2009). Third, as the effervescent atomisation utilises a small quantity of low-pressure gas for atomisation, it performs better than an air-assist or air-blast atomiser (Lefebvre, 1988; Jagannathan et al., 2011; Nielsen et al., 2006; Petersen et al., 2001) and is less sensitive to operating pressure (Jedelsky et al., 2003), reducing operating costs and increasing controllability with greater turndown ratios. Here air-assist or air-blast atomisers refer to atomizers where an additional air stream directed through the atomizer (as a separate coaxial stream) against the liquid sheet promotes the atomisation. In contrast, in effervescent atomizers, the gas is injected into the liquid stream to form a two-phase bubble flow which exits through a nozzle orifice.

Some disadvantages associated with effervescent atomisation are: (a) it requires a gas injection system, albeit at reasonably low pressure, which adds to the operation and design costs. (b) Due to the discontinuous nature of two-phase internal supply to the exit orifice, effervescent atomisation inherently produces a relatively unstable spray and a large range of droplet sizes, which in the extreme case can cause unwanted combustion characteristics like combustion instability, droplet clustering, noise and pollution (Sovani et al, 2001; Jicha et al., 2008; Luong et al., 2001; Liu et al., 2011). By fully understanding the effects of the

operating parameters on the internal flow and optimising the atomiser design, it is thought possible to minimise these undesirable effects.

There are two main configurations of aerators: (a) *inside-out* type and (b) *outside-in* type. In the former, the gas is injected through orifices located within a central tube (as depicted in Figure 1a). However, in the latter type, the gas-phase is injected from aerator orifices in the periphery of the mixing chamber (not shown here for brevity). The configuration employed in the present study is the *inside-out* type. A common aerator body design employed in the effervescent atomisers is *flat-end* cylindrical type.

A combination of *flat-end* type aerator body (Figure 1b) along with *inside-out* type aerator configuration poses a problem of ‘bluff body recirculation’ in effervescent atomisation. Bluff body recirculation is the generation of a reduced pressure zone in the downstream region of an aerodynamic body in a fluid flow. The *flat-end* aerator tube acts as a bluff body within the axial two-phase flow of the injected fluids. The gas injected gets trapped in the reduced pressure zone in the downstream wake and coalesce to form a cavity. The study of bluff body recirculation for axial flow across a cylinder applies to a surprisingly few numbers of scientific fields, being typically reported by research concerning projectiles (e.g., aeroplanes, submarines, torpedoes, missiles) (Saeidinezhad and Dehghan, 2005). Within these studies, flat-end cylinders were reported to have a significant wake effect i.e., high coefficient of drag compared to alternative drag reduced designs (Buresti et al., 1997). “Boat-tailing” is effective streamlining method, in which the cross section of the bluff body is gradually reduced to a tip – example designs referenced in the literature include: conical (Silhan and Cubbage, 1957), circular arc (Silhan and Cubbage, 1957), circular arc-conical hybrid (Mair, 1969; Buresti et al., 2007) and other intricate profiles like DARPA SUBOFF (Groves et al., 1989; Saeidinezhad and Dehghan, 2005; Peterson, 1981; Gross et al., 2011; Gross et al., 2013). An alternative well-known technique for base drag reduction is base-bleed, which features a flared base with ventilation cavities to promote axial fluid flow to the wake region (Viswanath, 1996). The only observation of bluff body recirculation effects in effervescent atomiser literature was in an internal flow visualisation study by Jobehdar (2014), in which the formation of a large gas void was observed to form in the wake region of a conventional flat-end aerator– this effect was reported to be mitigated by installing an arbitrary conical tip to streamline the aerator body (Figure 1b). The only other use of a streamlined aerator design is implied within the atomiser design drawings included by Hampel et al. (2009), but

it has not been studied as an independent variable. Therefore, the effect of bluff-body recirculation on inside-out effervescent atomisation is an under-researched area.

Next, a brief literature review of past studies describing internal two-phase flow inside effervescent atomizers is provided followed by a discussion of near-nozzle liquid breakup mechanisms. Given sufficient residence time, the injected gas-phase is stabilised within the mixing chamber to form patterns in the two-phase flow. In order to quantify the internal two-phase flow, these patterns are typically classified into common groups based on their visual appearance, termed 'flow regimes'. The standard flow regimes like bubbly flow, slug flow, churn flow, annular flow for vertical pipes are well described in two-phase flow literature. Bubbly flow is characterised by approximately uniformly-sized bubbles in a liquid continuum, which are significantly smaller than the mixing chamber and well dispersed, thus mitigating coalescence (Furukawa and Fukano, 2001; Zhou, 2013). For a study in vertically downwards orientation, Usui and Sato (1989) observed that bubbles tend to move towards the centre of the mixing chamber. Slug flow is the presence of Taylor bubbles i.e., hemispherical head and blunt tail end with smooth gas-liquid interface in a liquid continuum and of size similar to the mixing chamber diameter (Furukawa and Fukano, 2001; Zhou, 2013; Bhagwat, 2011). These large bubbles, commonly termed "slugs", are typically followed by a frothy wake of bubbles and are widely reported to be generated due to the coalescence of smaller bubbles (Zhou, 2013; Usui and Sato, 1989; Roesler and Lefebvre, 1987). As the probability of coalescence increases with bubble size, slug flow is thought to be instigated by the injection of sufficiently large gas entities at the aerator (Khirani et al., 2012).

Churn flow is a chaotic and oscillating flow regime, featuring disintegrated gas slugs without a hemispherical head shape (Zhou, 2013; Usui and Sato, 1989). The gas slugs are sufficiently large such that a peripheral liquid film is no longer constant and, therefore, neither phase can be considered continuous (Zhou, 2013). Annular flow is characterised by a liquid annulus about the mixing chamber periphery and a central gas core, where both liquid and gas phases are continuous (Furukawa and Fukano, 2001; Zhou, 2013). A small quantity of liquid entrainment may be present within the gas core due to shearing of the internal liquid-gas interface.

The near-nozzle liquid breakup mechanism in effervescent atomizers is different from that of single-phase atomiser (liquid only). [Specifically, the major destructive mechanism of liquid breakup leading to spray formation in single-phase atomizers is the turbulence of the](#)

liquid as it is discharged through the exit orifice (Lefebvre, 1989). The breakup response of an emerging liquid jet has been plotted by researchers in the parameter space of the Reynolds number (Re) and Ohnesorge number (Oh) (Ohnesorge, 1936; Reitz, 1978). The optimal spray is generated at the highest Reynolds and Ohnesorge numbers, whereby the liquid core is shattered into droplets immediately upon ejection from the orifice in a process termed “primary atomisation” (Ohnesorge, 1936). Consequently, single-phase atomisers are reliant on high liquid velocities through the exit orifice to generate sufficient turbulence for primary atomisation to be instigated.

In effervescent atomizers, a gas-phase is injected into the mixing chamber and, hence, a gas-liquid two-phase flow is supplied to the exit orifice. The presence of this gas-phase within generates further breakup mechanisms in addition to the single-phase atomisation mechanisms, which allows for forces external to the liquid to play a dominant role over turbulence (Sojka and Lefebvre, 1990). This reduces the dependency on high liquid velocities to generate primary atomisation (Chawla et al., 1985) and allows for two-phase atomisers to have a wider operating range with greater turn-down ratios (Jedelsky et al., 2013). Therefore, in an effervescent atomiser, the purpose of gas-phase injection is to aid primary atomisation. The presence of the gas-phase within the exit orifice acts to restrict the available flow area for the liquid phase (Sovani et al., 2001). This is further exacerbated due to the negative pressure differential across the nozzle, which causes the gas phase to expand. The expansion of gas phase produces dual effect. One, it further reduces the liquid flow area (Konstantinov, 2012), and second, it generates additional break-up mechanisms on the liquid-phase (i.e., increased aerodynamic Weber number (We)). Furthermore, as the liquid-phase is forced to flow through a significantly reduced peripheral fraction of the exit orifice (Lefebvre, 1988; Sovani et al., 2001), the liquid velocity is increased which also intensifies the turbulent breakup mechanism. Therefore, the gas-phase disruption has the benefit of increasing the performance of the atomiser (Lefebvre, 1989; Wang et al., 1989), where the droplet size produced is reported to be proportional to the square root of the ligament thickness (Lefebvre, 1988; Lefebvre, 1996).

Near nozzle spray structure emerging out of effervescent atomizers with internal flow regime of ‘bubbly type’ and ‘annular flow’ are discussed next as these are relevant in the present study. When the internal flow type is ‘annular flow’, an uninterrupted gas-phase is supplied to the exit orifice. In this case, liquid atomisation is aided by the continuous

aerodynamic shearing effect of the expanding gas-phase upon ejection from the exit orifice – this process is termed “tree regime atomisation” (Kim and Lee, 2001; Sovani et al., 2001; Santangelo and Sojka, 1995; Buckner and Sojka, 1991). Certain conditions have been reported to generate a thinner liquid annulus within the nozzle (e.g., increased ALR, decreased operating pressure), which has the effect of decreasing the “trunk” length and generating greater liquid breakup (Santangelo and Sojka, 1995). This compares to bubbly flow, which has the addition of an intermittent liquid-phase separating successive gaseous elements. The rapidly expanding gas upon ejection from the exit orifice has the effect of rupturing of the separating liquid-phase, in a non-continuous, explosion-like event termed “single bubble atomisation” (Lefebvre, 1988b; Kim and Lee, 2001; Santangelo and Sojka, 1995; Buckner and Sojka, 1991). Thus, the internal two-phase flow regime supplying the exit orifice has a significant effect on the two-phase atomisation processes.

The present experimental investigation is *Part I* of a two-part paper series which is concerned with study of internal flow field and near-nozzle spray visualisation employing flat-end and streamlined aerator bodies. The work presented here, for the first time, according to authors’ best knowledge, compares different streamlined aerator body designs to determine the best streamline design to produce favourable conditions for effervescent atomization i.e., ability to produce dense bubbly flow in the interior of the atomizer body over large operating condition range and the ability to rid the internal flow of aerator bluff body effects. *Part II* describes a detailed internal flow characterisation and spray characteristics of the best streamline aerator body determined in *Part I*. [The work described in both *Part I* and *Part II* have been reported in Ph.D. thesis of Niland \(2017\).](#)

2. Experimental setup and diagnostics

2.1 Test facility

The experimental test facility employed in the present study to visualise internal flow of an *inside-out* cylindrical effervescent atomiser is shown in Figure 2a. It consists of a transparent cylindrical mixing chamber within a cuboidal tank, with optical access gained through a window on each of the four major sides. To minimise refraction, the design exploits the “water tunnel” effect whereby the outer tank is filled with a liquid of refractive index similar

to the transparent mixing chamber and windows – in this case, a combination of acrylic glass (i.e., Perspex®) and water are selected (refractive index of acrylic glass: 1.50; refractive index of water: 1.33). The key advantage of adopting this design, as opposed to the solid transparent atomiser body demonstrated by Jobedhar (2014), is that it enables the mixing chamber to be interchanged without destructive machining processes on the atomiser body. The consequence of this passive refraction minimisation technique can be compared in Figure 2b and c, which shows the same scene of a checkerboard-insert within the cylindrical mixing chamber – a noticeable improvement in image distortion is achieved by comparing the results without (Figure 2b) and with water tunnel (Figure 2c) – particularly on the mixing chamber boundary.

An *inside-out* effervescent atomizer consists of an aerator tube placed inside a mixing chamber (Figure 2a). Different aerator tube designs (all of 10 mm diameter) are employed in the present study as explained later in this manuscript. The optical mixing chamber is cylindrical (diameter: 20 mm; mixing length: 325 mm). One of the objectives of the present study is to identify the stabilised flow regimes within the mixing chamber and hence it is advantageous to use a large mixing length to promote complete mixing. Fluid supply circuit to the effervescent atomiser is shown in Figure 2d. Liquid supply (water in the present study) is provided by a Lowara 3SV29F030T multistage centrifugal pump, which takes feed from a 1 m³ unsealed liquid (water) tank. The majority of the pump discharge is re-circulated to the liquid tank, with backpressure controlled by a gate valve. The liquid flow to the atomiser is controlled by a needle valve. The liquid mass flow rate, pressure and temperature respectively are measured by an Emerson Micromotion CMF 050 coriolis meter (LF in Figure 2d), a Druck PTX 1400 pressure transmitter (LP) and Type-K thermocouple (LT). Air is supplied up to 7 bar from an in-house compressed air line and the gas supply (Figure 2d) to the rig is controlled by a needle valve. The mass flow rate, pressure and temperature along the gas supply line are respectively measured by a Bronkhorst Cori-Tech M14V10I coriolis meter (GF), a Druck PTX 1400 pressure transmitter (GP) and Type-K thermocouple (GT). The operating pressure and temperature within the atomiser are measured with a Druck PTX 1400 pressure transmitter (AP) and Type-K thermocouple (AT) respectively. Flow is then discharged through a needle valve which, in addition to controlling the supply of liquid and gas to the rig, allows complete independent control of the fluid flow rates and

operating pressure. This arrangement is for all experiments in which internal flow is visualized by high-speed shadowgraphy (Figure 2d).

For the near-nozzle spray visualization and its characterizations (reported in *Part II* of this two-part series), [flow discharge is through exit orifices \(Figure 2d\)](#). Interchangeable exit orifices with diameters 1.0-2.0 mm having a common convergence angle of 45° (i.e. $2\beta=90^\circ$) are used to discharge the generated spray into the ambient atmosphere. The liquid flow rate is controlled by varying the exit orifice diameter between 1.0-2.0 mm. In the scenario where the discharge valve (needle valve) is employed to discharge the flow (internal flow visualisations experiments), different valve setting replicates different exit orifice diameters and different discharge valve settings along with variable input fluid flow rates are employed to control the flow.

All instrumentation data is acquired with a National Instruments DAQ data logger and transferred to a computer (Figure 2d). The signals are processed using National Instruments Signal Express, which also managed presentation and storage at 1 kHz sampling rate – the user is presented with data at 1 Hz frequency, enabling configuration of the experiment system to achieve the desired operating conditions. The sampling duration per test point is not controlled, but is typically in the order of 100 s. The data is post-processed to achieve average results and additional calculations are performed to generate non-measured data – for example, [Baker parameters \(Baker, 1954\) - Equations 1 and 2](#).

$$(G_l \Psi) = \frac{\dot{m}_l}{A_{MC}} \quad \text{Equation 1}$$

$$\left(\frac{G_g}{\lambda}\right) = \frac{\dot{m}_g}{A_{MC}} \quad \text{Equation 2}$$

Here, G_l and G_g are liquid (water in the present study) and gas (air in the present study) mass flux respectively (unit: kg/m²s). The quantities \dot{m}_l and \dot{m}_g represent liquid and gas mass flow rate (unit: kg/s). A_{MC} is mixing chamber cross-sectional area (m²). Quantities $\Psi = \left(\frac{\sigma_l}{\sigma_w}\right)^{-1} \left(\frac{\rho_l}{\rho_w}\right)^{-2.3} \left(\frac{\mu_l}{\mu_w}\right)^{1.3}$ and $\lambda = \sqrt{\left(\frac{\rho_g}{\rho_a}\right) \left(\frac{\rho_l}{\rho_w}\right)}$. These quantities basically normalise liquid and gas density (ρ), surface tension (σ) and dynamic viscosity (μ) correspondingly by water and air in case the liquid and gas considered are other than water and air. In the

present study water and air are employed as liquid and gas in the atomisation study and as such the quantities Ψ and λ are equal to unity.

The purpose of effervescent atomizer experiments reported in the present two-part study using water and air as liquid and gaseous medium respectively issuing into quiescent surrounding is to take first step towards understanding internal flow and spray characteristics of streamlined aerator configurations. The development of such an atomiser could be useful in many spray generation applications – for example, atomisation of various liquids in food or medical applications, controllable spray properties for fire suppression or incorporation of metallic flecks in spray paints. Future studies are planned with liquid and gas representing the actual spray applications.

2.2 Experimental diagnostics

High-Speed Shadowgraphy (Figure 3a) is used to observe the internal flow and near-nozzle atomisation. A Mikrotron MotionBLITZ Cube 2 high-speed camera is used in conjunction with a Navitar 16-160 mm zoom lens to record the flow. The camera is mounted on a computer controlled vertical traverse which allowed for accurate translation of the field of view, depending on the region of interest – for example, entire internal flow process for the internal flow visualisation and near nozzle flows for the spray characterisation. Backlighting is provided with two diffused 1000 W halogen light sources – these are positioned such that each light source provided sufficient and even lighting across the scene. Camera settings of 3000 Hz frame rate and 170 μ s shutter time are employed for internal flow visualisation whereas 1000 Hz frame rate and 30 μ s shutter time are employed to observe the near-nozzle atomisation mechanisms. These settings were experimentally determined to minimise image blurring, allow sufficient illumination and provide adequate time resolution to track the flow features.

Post-processing is applied to each of the measurement results to enhance the video. This is automated for each image within a video sequence using a purpose-written MATLAB computer script, as shown in Figure 3b.

3. Test cases and experimental conditions

Figure 4a shows different conventional flat-end aerator designs (A1-A4) employed in the present study. The outer tube diameter of all aerators is 10 mm. The difference between these aerator lies in the number of aerator holes on the surface and their diameters. The nomenclature ' $n \times \phi m$ ' is employed in Figure 4a for different aerators where ' n ' represents number of holes of diameter ' m ' which is in millimeters. All aerators have a fixed aeration area of 7.07 mm². To maintain a common aeration area with differing aerator orifice diameters, the aeration orifice configuration (e.g., number of orifices, hole positioning) was required to be varied among the investigated aerators – in general, the intention of the aerator designs was to maximise the orifice spacing within a 15 mm region and 10 mm from the aerator tip.

The liquid and gas delivery to the atomiser is discussed next. The sequence of fluid delivery to the atomiser for each test point is gas supply prior to liquid supply – this is thought to be in accordance with most industrial applications. The flow conditions are controlled by varying the discharge nozzle settings and the input fluid flow rates – this simulates two methods of turndown. Common discharge valve settings are achieved between investigations by adjusting the valve to specific flow rates at 0% ALR (i.e., 30, 60, 90, 120, 180, 240 and 290 g/s of liquid flow rates at 5 bar_g operating pressure) – each valve setting replicates a different exit orifice diameter and is consequently a method of turndown. The corresponding liquid Baker parameter (Equation 2) range is 95.5-923 kg/m²s. When using exit orifice for discharge (for spray characterisation) the liquid flow rate is controlled by varying the exit orifice diameter between 1.0-2.0 mm. The gas supply is varied in increments either up to the maximum achievable flow rate for the given aerator design (7 bar_g maximum supply pressure) or 5% ALR of 0.12, 0.25, 0.5, 1.0, 1.5, 2.0, 3.0, 4.0 and 5.0 %. The flow conditions are shown in Table 1. The stabilised two-phase internal flow and near-nozzle atomisation at each of these ALRs for every conventional flat-end aerator (Figure 4a) are imaged using High-Speed Shadowgraphy. Each test is repeated three times to determine repeatability.

Four streamlined aerator body designs (Figure 4b) are investigated in the present study to compare with conventional flat-end aerator designs mentioned above with respect to atomiser internal flow. These were selected from the literature as profiles with minimal

coefficient of drag. These are named as (a) 'CA' for 45° circular arc (Silhan and Cubbage, 1957) (b) 'H' for circular arc/conical hybrid (Mair, 1969) (c) 'C' for 16° conical (Silhan and Cubbage, 1957) and (d) 'A' for ADARPA (Groves et al., 1989). The name 'ADARPA' is used in the present study to denote a DARPA SUBOFF afterbody design employed in the existing literature (Groves et al., 1989). All four streamlined body designs are employed with aerator holes configuration A4 (Figure 4b). As such, the nomenclature (in Table 1) 'A4CA' represents 'CA' streamline aerator body with aerator holes configuration as in 'A4'. Having common aerator holes configuration for all four streamlined aerator body designs allows for a direct comparison between them. The identified differences between four streamlined designs are anticipated not to deviate much if other aerator hole configuration (A1, A2 and A3) are employed to compare between them and as such are not reported in the present study for brevity.

4. Results

Key experimental findings are discussed in two subsections. In the first section, unsuitability of conventional flat-end aerator body design for *inside-out* effervescent atomiser is demonstrated by investigating atomiser's internal flow. The unsuitability is primarily due to formation of a buoyant gas void within the aerator wake. In the next subsection, streamlined aerator body designs are employed to overcome the above limitation of gas void. In the process, four different streamlined aerator bodies are investigated to compare and contrast to determine the optimal one.

4.1. Internal flow visualisation of conventional flat-end aerator body effervescent atomiser

Figure 5 shows internal flow visualisation of *inside-out* effervescent atomiser employing different conventional flat-end aerators (mentioned in Section 2) at various ALRs. Only selected snapshots at some ALRs are shown here for brevity. It is observed that a large gas void is formed in the wake of all conventional flat-end aerators employed in the present study. This occurred for vertically downwards investigations at low ALRs ($< \sim 0.5\%$) from start-up. The formation of a gas void in this region is particularly problematic for effervescent atomisation as it is observed to displace the bubbles injected at the aerator

and therefore prevent formation of a conventional bubbly flow. An optimal effervescent atomiser configuration should enable bubbly flow across the widest range of fluid flow rates to enable stable spray generation and fine atomisation (Kim and Lee, 2001; Roesler and Lefebvre, 1987; Santangelo and Sojka, 1995; Buckner and Sojka, 1991; Roesler and Lefebvre, 1988). The gas void formation has been observed in the past (Jobedhar, 2014) where it was reported that its formation lead to decreased internal flow homogeneity, which eventually resulted in reduced spray stability. In the present work, it is shown that gas void is a common feature in the flow field for multitude of flat-end aerators and cannot be avoided in effervescent atomisers with flat-end aerators inclined vertically downwards at low ALRs ($< \sim 0.5\%$). It is interesting to note that this gas void formation is prevented in the wake of the aerator configuration A3 when the atomiser is operated in a vertically upwards orientation (Figure 6). Similar observations are made for other aerator configurations employed in the present study (not shown here for brevity). To authors' best knowledge, this is for the first time that the effect of atomiser orientation on the internal flow has been investigated.

Based on the above observations it is proposed that this gas void formation in vertically downward orientation can be explained by considering the restoring and detachment mechanisms acting on the gas-phase within the aerator wake region. To elaborate, the axial flow of liquid over the flat-end aerator cylindrical body generates significant bluff body recirculation which causes a reduced pressure region, within which the liquid viscous forces (e.g., drag, inertia), which aids in detachment of gas-phase, are reduced. In addition, the buoyancy acts opposite to the liquid drag in vertically downward orientation and is sufficient to overcome the viscous forces in the narrow aerator wake (Figure 6a). Thus, gas void finds favourable condition to establish itself at the aerator wake. Thus, buoyancy acts as restoring mechanism for gas void in vertically downward orientation. However, gas void is not observed under equivalent vertically upwards conditions because the gas-phase buoyancy now acts in the direction of liquid inertia (Figure 6b), as a result, there is no restoring mechanism acting on gas-phase to establish it in the aerator wake. This theory is corroborated in a supplementary experiment, in which a small quantity of gas is injected into an arbitrary liquid cross-flow (Figure 7). The injected gas entities can be seen to be "sucked" into the reduced pressure region existing within aerator wake, where all or some of the volume became "trapped". The trapped gas entities were seen to circulate in close

proximity, due to local pressure variations. It is known that prolonged bubble contact promotes coalescence (Yang et al., 2007; Tse et al., 1998; Laakkonen et al., 2006; Shinnar and Church, 1960) and, therefore, with increased gas-phase entrapment (i.e., increased ALR) and sufficient residence time, a gas void would be expected to be formed.

Next, a discussion of problems associated with the presence of gas void in the internal flow field of an effervescent atomiser is provided. The presence of gas void not only forces bubbles (injected at the aerator) to flow around the liquid periphery, thus preventing formation of a conventional bubbly flow which is desired in effervescent atomisers, but also, under certain conditions, produces unfavourable internal flow regimes. These include: (a) gas void disintegration to sparse polydispersed bubbles (Figure 8a) and (b) gas void disintegration to slug flows (Figure 8b). Each of these is explained in some detail as follows. In the first case (Figure 8a), the leading edge of a gas void disintegrates to form discrete bubbles in the downstream of flat end aerators. The process appears to be dominated by the bluff body effect of the gas void, in which high localised areas of reduced pressures are generated on the leading edge of the void causing chaotic ripping off of bubbles – this gas-phase break-up mechanism is in keeping with literature reports (Yang et al., 2007; Cheung et al., 2012). The bubbles (although sparse) generated in this manner are visibly different in size and thus are polydisperse. The point of void disintegration to bubbles is dependent on length of gas void which is sensitive to the operating conditions – rapidly growing when gas supply to the void (e.g., cavity forming, coalescence of bubbles) exceeds its depletion rate.

It is seen in the near-nozzle atomization visualizations (Figure 9) that, if the gas void grows to exceed the length of the mixing chamber, uninterrupted gas-phase is supplied to the exit orifice –the spraying mechanism becomes *tree-regime atomisation* (Figure 9; $t=0.008$ s). This type of atomisation has been identified in past (Santangelo and Sojka, 1995; Buckner and Sojka, 1991) in which liquid atomisation is aided by the continuous aerodynamic shearing effect of the uninterrupted expanding gas-phase upon ejection from the exit orifice. The tree-regime atomisation, however, is temporary as the void rapidly drains of gas-phase, whereby its length reduces and the supply to the exit orifice is now sparse polydisperse bubble flow (Figure 9; $t=0$ s, $t=.004$ s and $t=0.016$ s). The atomisation mechanism now becomes single *bubble atomisation*. This type of atomisation is different from the tree-regime atomisation in the sense that the dispersion of bubbles in the liquid generates intermittent liquid-phase separating successive gaseous elements. The gas expands rapidly

upon ejection from the exit orifice and ruptures the separating liquid-phase, in a non-continuous, explosion-like event.

It is thus clear from Figure 9 that operation with gas void disintegration to sparse bubbly flow is not recommended as gas supply to the exit orifice can rapidly switch between the polydisperse bubbles and uninterrupted gas void thus generating different spray characteristics which can lead to spray instability. An unstable spray is undesirable for the majority of considered applications, due to generation of fluctuating spray properties – this causes a greater range of droplet sizes, whereby fine droplets alternate with the formation of larger ligaments (Schröder et al., 2011).

The next unfavourable internal flow discussed is gas void disintegration to slug flows (Figure 8b). Passing gas entities injected from the aerator are observed to interfere with the void generating surface instabilities on the gas-liquid interface. This is seen to be encouraged by the presence of large bubbles or jets in the liquid periphery. Under critical conditions, this is seen to either completely detach the gas void from the aerator tip or rip volumes of gas from the void within the mixing chamber. Figure 10 shows atomisation of a gas void disintegrated slug flow. These slugs are interspersed with bubbles, which are injected from the aerator and initially forced to flow around the liquid periphery of the void. Consequently, the gas entities supplying the exit orifice vary between bubbles and slugs – therefore the spray generation is single bubble atomisation intermixed with erratic tree regime atomisation. Therefore, the spray, as before, is observed to be unstable.

To summarise, gas void is observed to be formed in the wake of a conventional flat-end aerator for all vertically downwards investigations. This is caused by the buoyancy of the gas-phase overcoming the liquid shear within the aerator wake, due to the bluff body recirculation effect of the axial flow across the aerator body. The formation of a void in this region is observed to be particularly problematic for effervescent atomisation, as it is seen to displace any injected bubbles and, therefore, prevent a bubbly flow in the interior of an effervescent atomiser. In addition, void disintegration to polydisperse bubbles and slugs results in unstable spray. The effects of increased liquid flow rate (up to 290 g/s), decreased mixing chamber diameter (from 14 mm diameter, corresponding to a maximum liquid Baker parameter of 1880 kg/m²s) or increased operating pressure (up to 5 bar) are unable to displace the gas void. This is tested in the present study and is not reported here for brevity.

4.2. Internal flow studies of streamlined aerator body effervescent atomisers

An alternative solution to detach the void is to reduce the bluff body recirculation effect of the aerator body, for example with streamlined tips – this was reported to be an effective solution by Jobedhar (2014), who studied the effect of an arbitrary conical end tip. In this subsection, internal flow of streamlined aerator effervescent atomisers is visualised to show the absence of gas void and hence advantageous over conventional flat-end aerator design. To this effect, it is important to evaluate both start-up and running conditions. Specifically, an aerator body must (a) get rid of gas void or ambient air upon start-up and (b) once running, it should prevent the formation of gas void within the mixing chamber. Each of these aspects is discussed in detail now. Subsequently, the best among the four streamlined designs is evaluated based on (a) ability to produce desirable bubbly flow inside the effervescent atomiser and (b) ability to produce minimum wake-effect.

4.2.1. Absence of gas void in streamlined aerator body effervescent atomisers

Four streamlined aerator body designs are investigated for their ability to passively bleed the mixing chamber of ambient air upon start-up, in which the effervescent atomiser is initially under atmospheric conditions (i.e., the mixing chamber evacuated of liquid and occupied with ambient air). Liquid is then suddenly supplied to the atomiser ranging from 30 – 289 g/s (with corresponding liquid Baker parameter 95.5 – 923 kg/m²s), with the discharge valve setting controlled to maintain 5 bar operating pressure. Liquid supply is varied systematically in steps in different start-up trails.

It is observed that all streamlined aerator tips considered in the present study are consistently able to passively bleed the mixing chamber from start-up for liquid flow rates above ~75 g/s (corresponding to a liquid Baker parameter of 239 kg/m²s) as shown in Figure 11a. This is due to having sufficiently low bluff body recirculation, and the clearing ambient air has sufficiently high momentum, to prevent gas-phase from becoming entrapped within the aerator wake and forming a gas void. This contrasts to the conventional flat-end aerator (Figure 11b), which features a gas void in the aerator wake upon identical start up conditions. Although other flat-end aerators were also tested from start-up, only 'A4' profile is reported here for brevity.

It is also observed that all the streamlined aerator tips did not succeed in bleeding the mixing chamber of the ambient air below a liquid flow rate of $\sim 75 \text{ g/s}$ (corresponding to a liquid Baker parameter of $239 \text{ kg/m}^2\text{s}$). This situation is thought to occur when the liquid shear around the aerator periphery is insufficient to overcome the buoyancy of the ambient air and displace it from above the aerator. Although streamlined aerator bodies succeeded in bleeding the mixing chamber of ambient air beyond liquid Baker parameter of $239 \text{ kg/m}^2\text{s}$, however, these observations are still of significant importance because the conventional flat-end aerators were unable to prevent gas void formation under any of the tested conditions. Thus, within the test conditions employed in the present study it is concluded that the streamlined aerator body designs are advantageous over conventional flat-end aerator bodies between liquid Baker parameter range $239 - 923 \text{ kg/m}^2\text{s}$ which is still a significantly large range.

Next, the internal flow field when the aerator is in running condition is considered (i.e., both gas and liquid flows present). Example comparisons between the conventional flat-end and ADARPA aerator body designs are provided for equivalent operating conditions in Figure 12. Other streamlined aerators are not shown here for brevity. These observations are made for liquid flow rate of $75 - 289 \text{ g/s}$ (liquid Baker parameter range: $239 - 923 \text{ kg/m}^2\text{s}$) and ALR of $0 - 0.5\%$. It is observed that for vertically downward orientation the effects of the reduced bluff body recirculation effect for the streamlined case prevents the formation of gas void in the aerator wake. However, at similar operating conditions the conventional flat-end aerators favoured the formation of gas void. Vertically upward flow is also shown in Figure 12 to confirm that gas void is not formed in both streamlined aerator tip flow field and conventional flat-end aerator flow (as described in the previous subsection).

4.2.2. Evaluation of best streamlined aerator design

It was shown that all the four streamlined aerator tip designs considered in the present study succeeded in preventing the formation of undesirable gas void in the aerator wake. In this section, these streamlined aerator designs are evaluated to determine the best. It is known that the purpose of an effervescent atomiser aerator is to inject the gas-phase into the liquid-phase to form uniformly sized bubbles and, hence, generate a homogenous dense bubbly flow (Kim and Lee, 2001; Roesler and Lefebvre, 1987; Santangelo and Sojka, 1995;

Buckner and Sojka, 1991; Roesler and Lefebvre, 1988). Consequently, bubbly flow can be expected when gas injection from the aerator is in the form of monodisperse bubbles.

Figure 13 compares the operating ranges over which bubbly flow is achieved for four streamlined aerator designs considered in the present study. The co-ordinate space over which bubbly flow is observed in the interior of the mixing chamber in the effervescent atomiser considered in the present study is shown with shaded region. It is observed (Figure 13) that, for all the geometries, the bubbly flow region is not observed at: (a) High ALRs i.e., $ALR > \sim 0.5$, the bubbles transitioned to jets/large size bubbles at higher ALRs; (b) Low liquid flow rates (i.e., $< \sim 70 \text{ g/s}$), due to the high relative effects of buoyancy compared to viscous forces. Under these conditions, the gas-phase has greater residence time in the mixing chamber which increases the gas-phase coalescence. Consequently, injected bubbles and jets are observed to coalesce within the mixing chamber to form disturbed annular and annular flows; and (c) High liquid flow rates (i.e., $> \sim 290 \text{ g/s}$), by the flow limit of the discharge valve.

However, it is observed that among the considered streamline geometries, the ADARPA aerator is determined to have a marginally larger bubbly flow region. The ability of an aerator to produce homogenous and dense bubbly flow resulting in favourable spray characteristics is determined as follows: a region in the parameter space of gas mass flow rate (ordinate) and liquid mass flow rate (abscissa) is drawn which represent all flow setting combinations (gas and liquid mass flow rates) which produce desired dense bubbly and bubbly-slug flow regimes. The area of the region is called as bubbling operating range ($OR_{bubbling}$) with units g^2/s^2 . The magnitude of $OR_{bubbling}$ directly relates to the ability of an aerator to produce desired flow regimes. Aerators with higher $OR_{bubbling}$ would be preferred over their peers having lower $OR_{bubbling}$. Bubbling operating range for different streamlined aerator bodies are shown in Figure 14 where it is seen that $OR_{bubbling}$ is $\sim 20\%$ more for ADARPA than the other three streamlined profiles considered in the present study. Although the bubbly flow production range for ADARPA is only marginally higher than other streamline profiles, the ADARPA is concluded to be the best among four geometries because it has minimum wake effect. To prove this, a comparison of the ability of the aerator body designs to remove an established gas void is made. To elaborate, it was reported in previous sub section that gas void was not formed in streamlined aerator body effervescent atomisers within a test range (of the present study) of $75 - 289 \text{ g/s}$ (liquid Baker

parameter range: $239 - 923 \text{ kg/m}^2\text{s}$). Thus, it is envisaged that if a gas void is deliberately maintained at flow rates below 75 g/s of liquid flow ($< 239 \text{ kg/m}^2\text{s}$) and ability of aerator body designs to remove this gas void is evaluated by systematically increasing the liquid flow rate in steps, then the aerator which can rid the internal flow of gas void at minimum liquid flow rate beyond $\sim 75 \text{ g/s}$ is the aerator tip with minimum wake effect.

Unlike the previous test, the discharge valve is kept fully open and, therefore, the operating pressure is not controlled by altering the settings of the discharge valve. A gas void is successfully established in the wake region of each aerator at a liquid flow rate of 50 g/s such that the gas-phase found equilibrium at the aerator tip to form a gas void. The liquid flow rate is gradually increased (thereby increasing the atomiser pressure) by approximately 1 g/s increments in 10 seconds intervals until either the gas void is detached from the aerator tip or the maximum 5 bar gauge operating pressure is reached (corresponding to a maximum liquid mass flow rate of 289 g/s and liquid Baker parameter of $923 \text{ kg/m}^2\text{s}$). The results are shown in Figure 15. It is observed that the ADARPA aerator tip required the lowest liquid flow rate (almost just above 75 g/s – with atomiser pressure of 0.3 bar_g) of all the investigated aerator body designs to detach an established gas void from the aerator wake region and is, therefore, considered to have the lowest wake effect for use as an aerator body design in inside-out effervescent atomiser. Both the flat-end and circular arc designs are shown (Figure 15) to prevent gas void detachment across all conditions tested, including at the highest investigated liquid flow rate – however, the circular arc design was previously shown to passively bleed the atomiser at flow rates far below this. Therefore, it is concluded that out of the four streamline profiles employed in the present study, the ADARPA design is the most suitable for use in effervescent atomisers whereas ‘Circular arc’ design is least suitable.

5. Conclusion

An experimental investigation visualizing the internal flow of an *inside-out* type effervescent atomizer using high-speed shadowgraphy was conducted. A comparison between internal flow of effervescent atomizer employing conventional flat-end aerator body and four different streamlined aerator body designs was made. Four types of streamlined aerator body tips had the shape of circular arc, circular arc/conical hybrid, conical and DARPA SUBOFF afterbody design which is termed “ADARPA” within this work.

The air-to-liquid ratio (ALR) was investigated in 0-5% range with the operating pressure maintained constant at 5 bar. The liquid Baker parameter was maintained in the range $95.5 - 923 \text{ kg/m}^2\text{s}$. It was observed that when the flow in the effervescent atomizer was in vertically downwards direction, a gas-void was formed in the wake of the conventional flat-end aerator body due to significant bluff-body recirculation which caused a reduced pressure region. This reduced pressure was characterized by reduced liquid viscous forces as compared to buoyancy and the latter overcame the former to support the maintenance of gas void in the aerator wake. The gas-void, however, was not observed in the internal flow employing any of the streamlined aerator bodies in the liquid Baker parameter range of $239 - 923 \text{ kg/m}^2\text{s}$. This was due to reduction of the bluff body recirculation effect of the streamlined aerator body. Neither was it observed in the conventional flat-end aerator body when the flow was maintained in the upward direction.

The problems associated with the existence of gas-void was observed to be due to disintegration of gas-void to either sparse polydispersed bubbles or to slug flows before the orifice exit. Such disintegration resulted in near-nozzle liquid breakup mechanism to fluctuate between *tree-regime* type and *single bubble atomization* type. This resulted in undesirable fluctuation in the spray properties.

Next, four streamlined aerator body designs were evaluated to determine the best among them with respect to the ability of these aerator bodies to get rid of gas void or ambient air upon start-up and once running, the ability to prevent the formation of gas void within the mixing chamber. It was observed that, within the tested conditions in the present study, the DARPA SUBOFF afterbody design performed the best with its ability to produce desirable bubbly flow inside the effervescent atomiser over relatively large flow conditions owing to its ability to produce minimum wake-effect.

References

- Baker, O., New pipeline techniques designing for simultaneous flow of oil and gas. *The Oil and Gas Journal*, vol. 53(12), pp. 185-195, 1954
- Bhagwat, S.M., Study of flow patterns and void fractions in vertical downward two phase flow, PhD, Oklahoma State University, 2011.
- Buckner, H.N. and P.E. Sojka, Effervescent Atomization of high-viscosity fluids: Part I. Newtonian Liquids, *Atomization and Sprays*, vol. 5 no. 2, pp. 137-155, 1995.
- Buresti, G., R. Fedeli, and A. Ferraresi, Influence of afterbody rounding on the pressure drag of an axisymmetrical bluff body, *Journal of Wind Engineering and Industrial Aerodynamics*, vol. 69, pp. 179-188, 1997
- Buresti, G. Iungo, G. Lombardi, Methods for the drag reduction of bluff bodies and their application to heavy road-vehicles, 1st Interim Report Contract between CRF and DIA DDIA2007-6, 2007.
- Catlin, C.A. and J. Swithenbank, Physical processes influencing effervescent atomizer performance in the slug and annular flow regimes, *Atomization and Sprays*, vol. 11, no. 5, pp. 575-595, 2001.
- Chawla, J.M., Atomisation of Liquids employing the Low Sonic Velocity in Liquid/Gas Mixtures, 3rd International Conference on Liquid Atomisation and Spray Systems, London, UK, 1985.
- Cheung, S.C.P., Yeoh, G.H., Qi, F.S., Tu, J.Y., Classification of bubbles in vertical gas-liquid flow: Part 2 - A model evaluation, *International Journal of Multiphase Flow*, vol. 39: p. 135-147, 2012.
- Furukawa, T. and T. Fukano, Effects of liquid viscosity on flow patterns in vertical upward gas-liquid two-phase flow, *International Journal of Multiphase Flow*, vol. 27, no. 6, pp. 1109-1126, 2001.
- Gosselin, P.G., Lund, M.T., Sojka, P.E., Lefebvre, A.H., Consumer product package incorporating a spray device utilizing large diameter bubbles, US Patent 5,323,935, filed Feb 21, 1992, and issued Jun 28, 1994.
- Gross, A., A. Kremheller, and H. Fasel. Simulation of flow over SUBOFF bare hull model, 49th AIAA aerospace sciences meeting, Orlando, Florida, USA, 2011.

- Gross, A., C. Jagadeesh, and H.F. Fasel, Numerical and experimental investigation of unsteady three-dimensional separation on axisymmetric bodies, *International Journal of Heat and Fluid Flow*, vol. 44, pp. 53-70, 2013.
- Groves, N.C., T.T. Huang, and M.S. Chang, Geometric Characteristics of DARPA (Defense Advanced Research Projects Agency) SUBOFF Models, David Taylor Research Center, Ship Hydromechanics Department, Report Number DTRC/SHD-1298-01, 1989.
- Hampel, U., Othál, J., Boden, S., Beyer, M., Schleicher, E., Zimmermann, W., Jicha, M., Miniature conductivity wire-mesh sensor for gas-liquid two-phase flow measurement, *Flow Measurement and Instrumentation*, vol. 20, no. 1, pp. 15-21, 2009.
- Jagannathan, T.K., R. Nagarajan, and K. Ramamurthi, Effect of ultrasound on bubble breakup within the mixing chamber of an effervescent atomizer, *Chemical Engineering and Processing: Process Intensification*, vol. 50, no. 3, pp. 305-315, 2011
- Jedelsky, J., M. Jicha, and J. Slama, Characterization of spray generated by multihole effervescent atomizer and comparison with standard Y- jet atomizer, *Proc. of the Ninth International Conference on Liquid Atomization and Spray Systems (ICLASS-2003)*, Sorrento, Italy, 2003.
- Jedelsky, J., Miroslav, J., Slama, J. and Otahal, J., Development of an effervescent atomizer for industrial burners, *Energy and Fuels*, vol. 23, no. 12, pp. 6121-6130, 2009.
- Jicha, M. and J. Jedelsky, Unsteadiness in effervescent sprays: A new evaluation method and the influence of operational conditions, *Atomization and Sprays*, vol.18, no. 1, pp. 49-83, 2008.
- Jobehdar, M.H., Experimental Study of Two-Phase Flow in a Liquid Cross-Flow and an Effervescent Atomizer, PhD, University of Western Ontario, 2014.
- Khirani, S., Kunwapanitchaku, P., Augier, F., Guiui, C., Guiraud, P., Hebrard, G., Microbubble generation through porous membrane under aqueous or organic liquid shear flow, *Industrial and Engineering Chemistry Research*, vol. 51, no. 4, pp. 1997-2009, 2012.
- Kim, J.Y. and S.Y. Lee, Dependence of spraying performance on the internal flow pattern in effervescent atomizers, *Atomization and Sprays*, vol. 11, no. 6, pp. 735-756, 2001.
- Konstantinov, D.D., Effervescent Atomisation for Complex Fuels including Bio-Fuels, PhD, University of Wales Cardiff, 2012.

- Laakkonen, M., V. Alopaeus, and J. Aittamaa, Validation of bubble breakage, coalescence and mass transfer models for gas-liquid dispersion in agitated vessel, *Chemical Engineering Science*, vol. 61, no. 1, pp. 218-228, 2006.
- Lefebvre, AH., Wang, XF., Martin, CA., Spray characteristics of aerated-liquid pressure atomizers, *AIAA J Prop Power.*, vol. 4, no. 4, pp. 293-298, 1988.
- Lefebvre AH., A novel method of atomization with potential gas turbine application, *Defence Science Journal*, vol. 38, pp. 353-361, 1988.
- Lefebvre, A.H., *Atomization and sprays*, London: Taylor & Francis, 1989.
- Lefebvre, A.H., Some recent developments in twin-fluid atomization, *Particle and Particle Systems Characterization*, vol. 13, no. 3, pp. 205-216, 1996.
- Liu, M., Duan, Y., Zhang, T. and Xu, Y., Evaluation of unsteadiness in effervescent sprays by analysis of droplet arrival statistics - The influence of fluids properties and atomizer internal design, *Experimental Thermal and Fluid Science*, vol. 35, no. 1, pp. 190-198, 2011.
- Lörcher, M., F. Schmidt, and D. Mewes, Effervescent atomization of liquids, *Atomization and Sprays*, vol. 15, no. 2, pp. 145-168, 2005.
- Luong, J.T.K. and P.E. Sojka, Unsteadiness in effervescent sprays, *Atomization and Sprays*, vol. 9, no. 1, pp. 87-109, 1999.
- Mair, W., Reduction of base drag by boat-tailed afterbodies in low-speed flow, *Aeronautical Quarterly*, vol. 20, no. 4, pp. 307-320, 1969.
- Nielsen, A.F., Poul, B., Kristensen, H.G., Kristensen, J., Hovgaard, L., Investigation and comparison of performance of effervescent and standard pneumatic atomizer intended for soluble aqueous coating, *Pharmaceutical Development and Technology*, vol. 11, no. 2, pp. 243-253, 2006.
- [Niland, A., Internal flow studies for the characterisation and optimisation of an effervescent atomiser, PhD Thesis, Cardiff University, 2017.](#)
- [Ohnesorge, W., Formation of drops by nozzles and the breakup of liquid jets, Z. Angew. Math. Mech., Vol. 16, 1936, pp. 355–358.](#)
- Peterson, R.L., Drag Reduction Obtained by the Addition of a Boattail to a Box Shaped Vehicle, NASA CR-163113 MS Thesis, Aug, 1981.

- Petersen, F.J., Worts, O., Schaefer, T., Sojka, P.E., Effervescent atomization of aqueous polymer solutions and dispersions, *Pharmaceutical Development and Technology*, vol. 6, no. 2, pp. 201-210, 2001.
- Reitz, R. D., *Atomization and Other Breakup Regimes of a Liquid Jet*, Ph.D. thesis, Princeton University, Princeton, NJ, 1978
- Roesler TC. and Lefebvre, AH., Studies on aerated-liquid atomization. *Int J Turbo Jet Engines.*, vol. 6, pp. 221-230, 1989.
- Saeidinezhad, A. and A.A. Dehghan, Nose shape effect on the visualized flow field around an axisymmetric body of revolution at incidence, *Journal of Visualization*, vol. 18, no. 1, pp. 83-93, 2015.
- Santangelo, P.J. and P.E. Sojka, A Holographic Investigation of the near-nozzle structure of an Effervescent atomizer-produced spray, *Atomization and Sprays*, vol. 5 no. 2, pp. 137-155, 1995.
- Schröder, J., Kraus, S., Rocha, B.B., Gaukal, V., Schuchmann, H.P., Characterization of gelatinized corn starch suspensions and resulting drop size distributions after effervescent atomization, *Journal of Food Engineering*, vol. 105, no. 4, pp. 656-662, 2011.
- Shinnar, R. and J.M. Church, Statistical Theories of Turbulence in Predicting Particle Size in Agitated Dispersions, *Industrial & Engineering Chemistry*, vol. 52, no. 3, pp. 253-256, 1960.
- Silhan, F.V. and Cabbage, J.M Jr., Drag of Conical and Circular-Arc Boattail Afterbodies at Mach Numbers From 0.6 to 1.3, National Advisory Committee for Aeronautics, Washington, Tech. Rep. RM-L56K22, Jan. 1957.
- Sojka, P.E. and A.H. Lefebvre, A Novel Method of Atomizing Coal-Water Slurry Fuels, US DOE, Pittsburgh, Tech. Rep. DOE/PC/79913-T4, May 1990.
- Sovani, S.D., P.E. Sojka, and A.H. Lefebvre, Effervescent atomization, *Progress in Energy and Combustion Science*, vol. 27, no. 4, pp. 483-521, 2001.
- Sovani, S.D., Chou, E., Sojka, P.E., Gore, J.P., Eckerle, W.A., Crofts, J.D., High pressure effervescent atomization: Effect of ambient pressure on spray cone angle, *Fuel*, vol. 80, no. 3, pp. 427-435, 2001.

- Tse, K., Martin, T., Mcfarlane, C.M., Nienow, A.W., Visualisation of bubble coalescence in a coalescence cell, a stirred tank and a bubble column, *Chemical Engineering Science*, vol. 53, no. 23, pp. 4031-4036, 1998.
- Usui, K. and K. Sato, Vertically downward two-phase flow, (I) Void distribution and average void fraction, *Journal of Nuclear Science and Technology*, vol. 26, no. 7, pp. 670-680, 1989.
- Viswanath, P., Flow management techniques for base and afterbody drag reduction, *Progress in Aerospace Sciences*, vol. 32(2), pp. 79-129, 1996.
- Wang, XF., Chin, JS. and Lefebvre, AH. Influence of gas injector geometry on atomization performance of aerated-liquid nozzles, *Int J Turbo Jet Engines*, vol. 6, pp. 271-280, 1989.
- Yang, G.Q., B. Du, and L.S. Fan, Bubble formation and dynamics in gas-liquid-solid fluidization- A review, *Chemical Engineering Science*, vol. 62, no.1-2: pp. 2-27, 2007.
- Zhou, J., Flow patterns in vertical air/water flow with and without surfactant, PhD, University of Dayton, 2013.

Figures and Tables

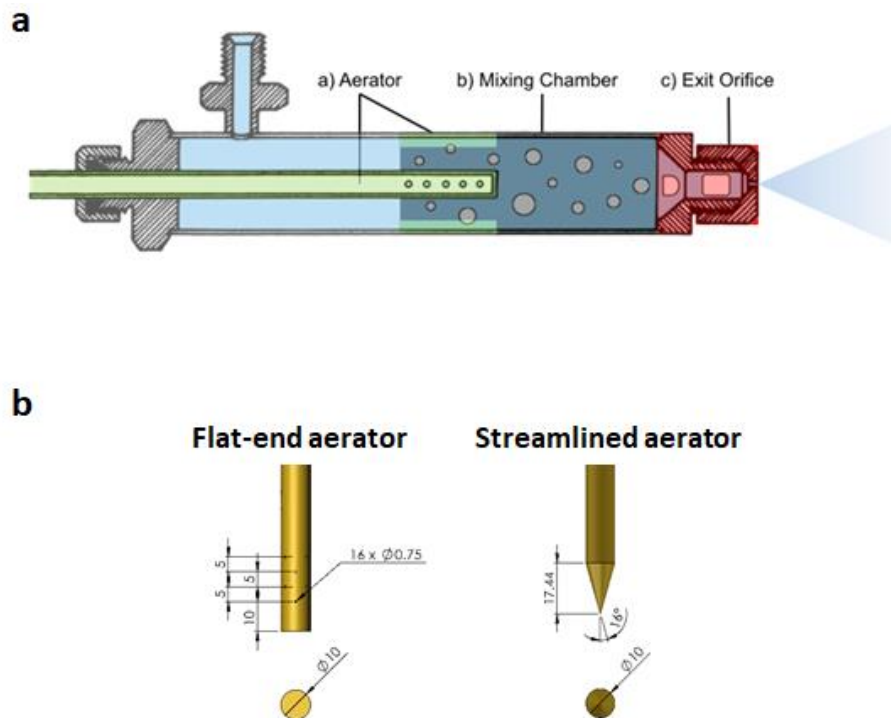


Figure 1(a) Effervescent atomiser common components. (b) Aerator body designs

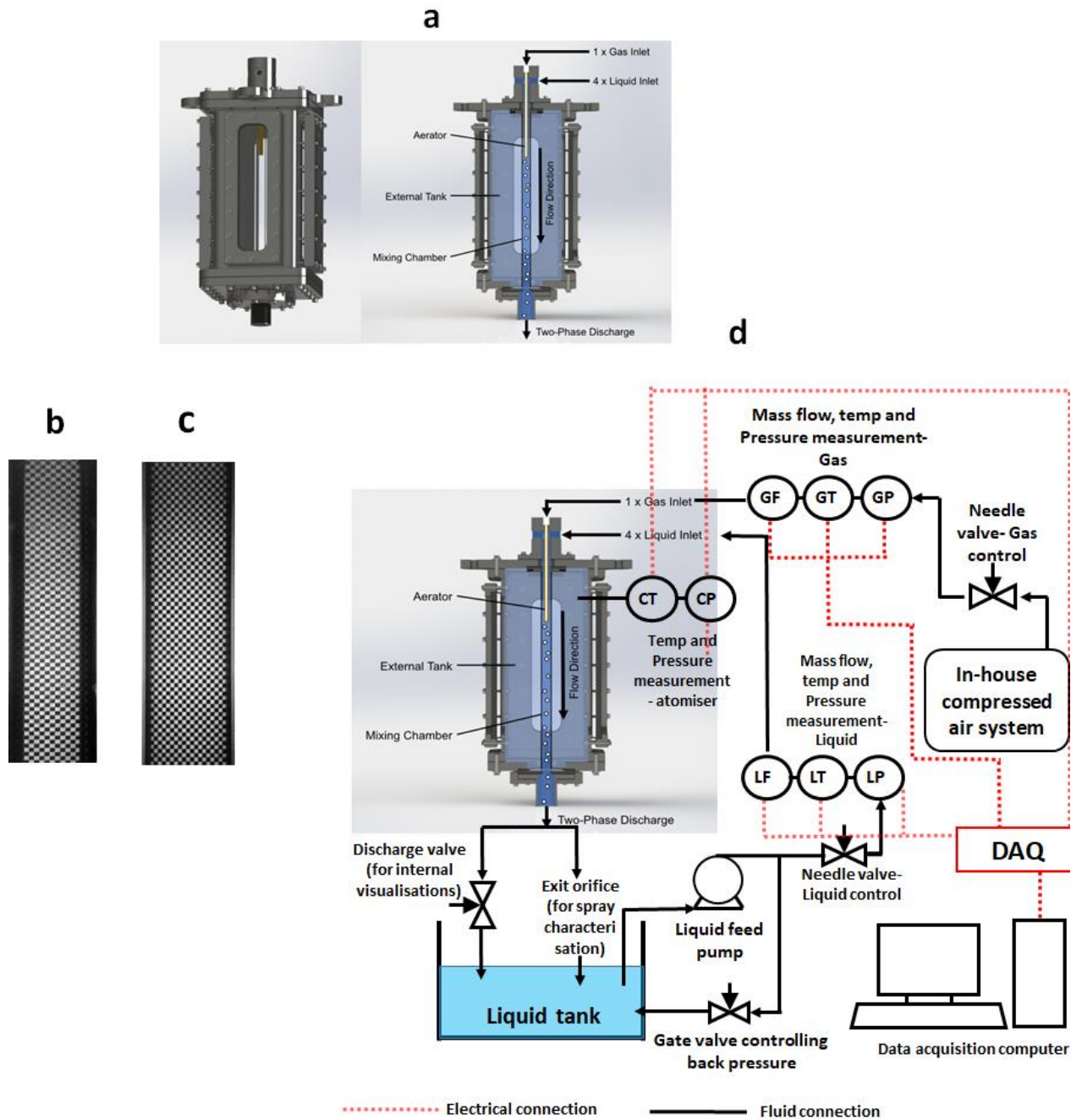


Figure 2. Experimental test facility and fluid flow circuit employed in the present effervescent atomiser study (a) effervescent atomizer with aerator and mixing chamber; (b) Image distortion through a cylindrical mixing chamber without refraction minimisation; (c) image with water tunnel (d) fluid supply lines and its controllers

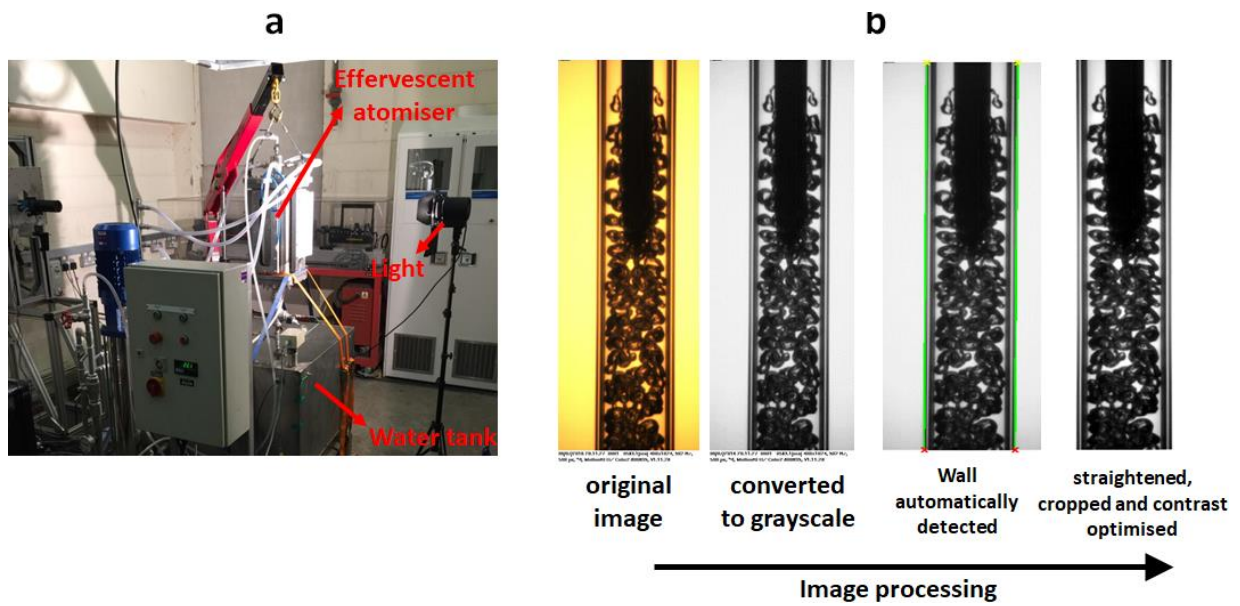
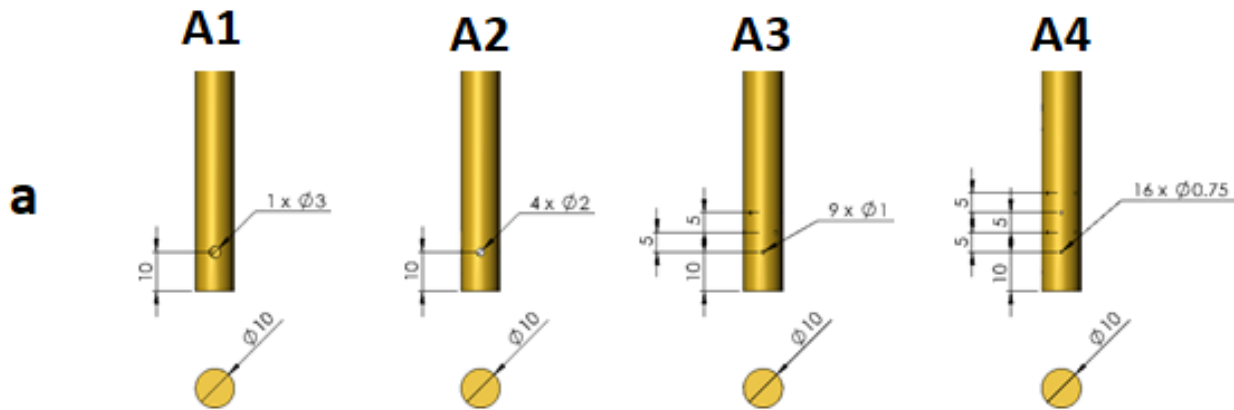


Figure 3. (a) High speed shadowgraphy set up; (b) Sequence of image processing applied to internal flow visualisation images obtained from high speed shadowgraphy.

Conventional flat-end aerator designs



Streamlined aerator designs

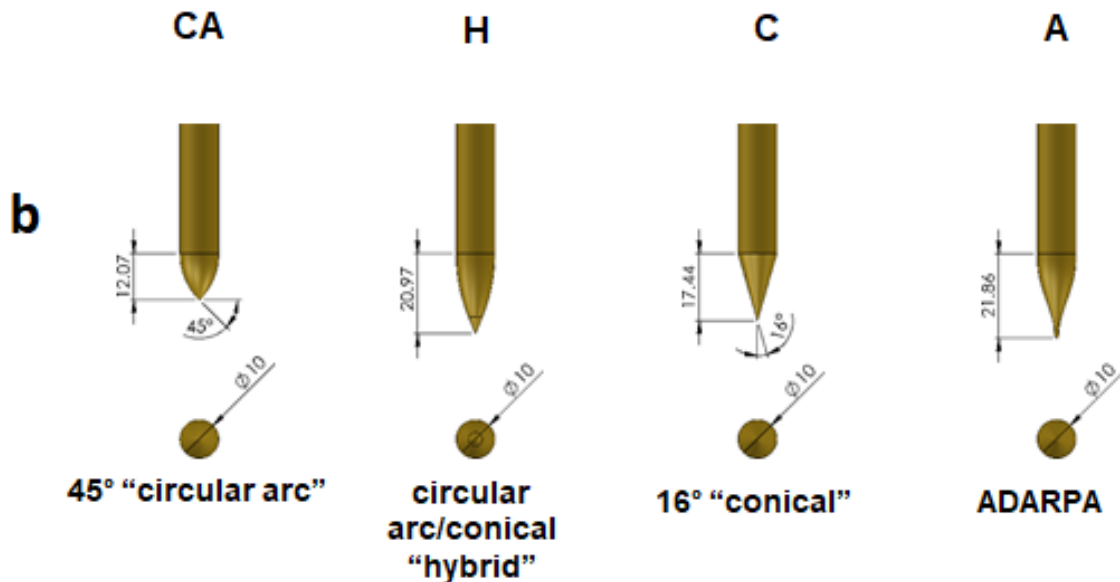


Figure 4. (a) Conventional flat-end aerator designs employed in the present study (dimensions in mm) (b) Streamlined aerator body designs (dimensions in mm): CA – 45° "circular arc" (Silhan and Cubbage, 1957); H – circular arc/conical "hybrid" (Mair, 1969); C – 16° "conical" (Silhan and Cubbage, 1957); A – "ADARPA" (Groves et al., 1989).

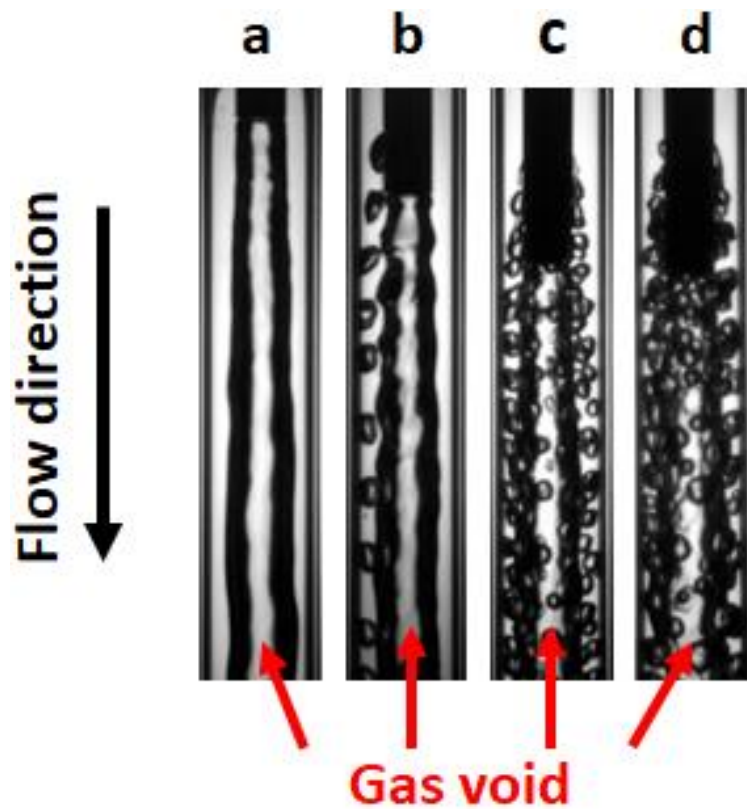


Figure 5. Example observations of gas void formation in aerator wake for different aerator configurations: (a) Configuration: A1; ALR: 0.02% (b) Configuration: A2; ALR: 0.03% (c) Configuration: A4; ALR: 0.13% (d) Configuration: A4; ALR: 0.25%.

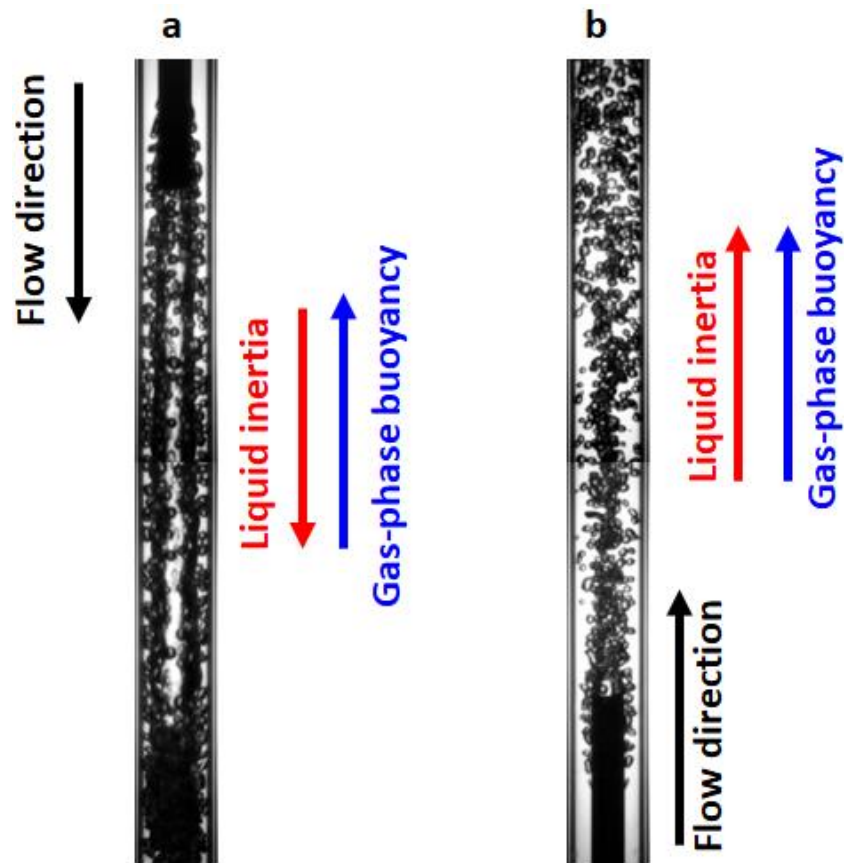


Figure 6. Example observation of effect of orientation at comparable ALR and fully open discharge nozzle setting (i.e. equivalent exit orifice diameter) for A3 configuration: (a) Vertically downwards, 0.13% ALR (b) Vertically upwards, 0.12% ALR.

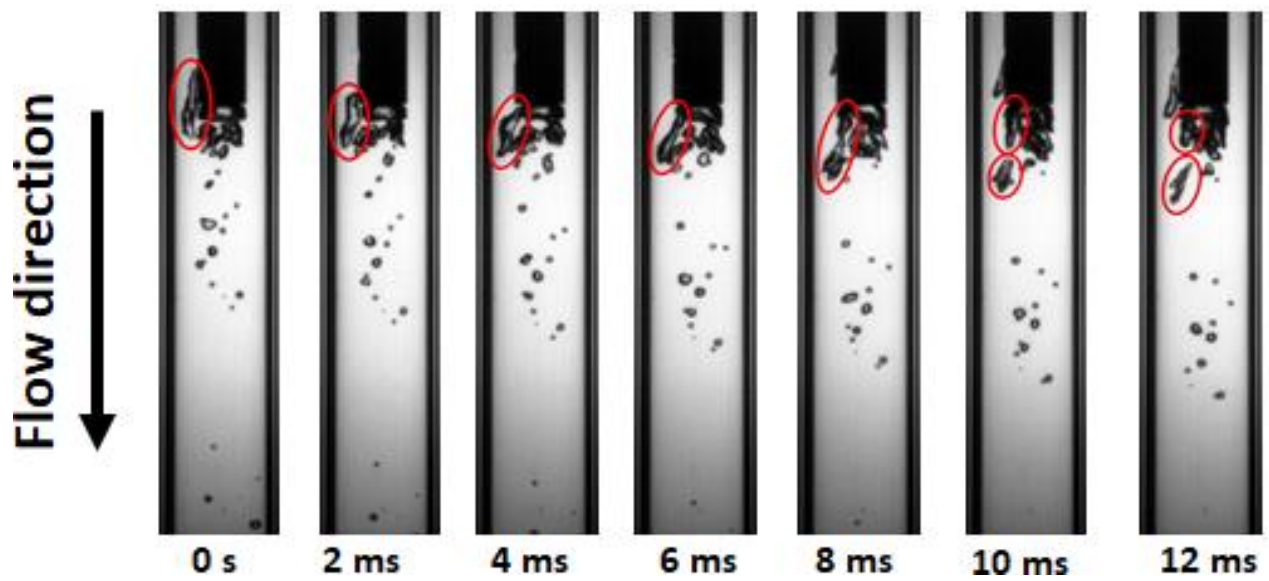


Figure 7. Observation of gas entity entrapment in aerator wake from bled start-up (ALR: 0.003%)

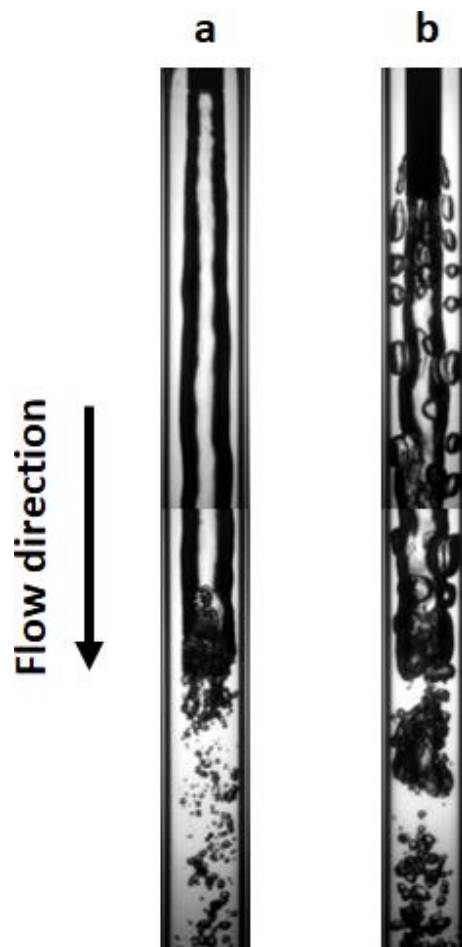


Figure 8. Examples of gas void shearing: a) Liquid Baker parameter: $742 \text{ kg/m}^2\text{s}$, 0.002% ALR;
b) Liquid Baker parameter: $605 \text{ kg/m}^2\text{s}$, 0.41% ALR

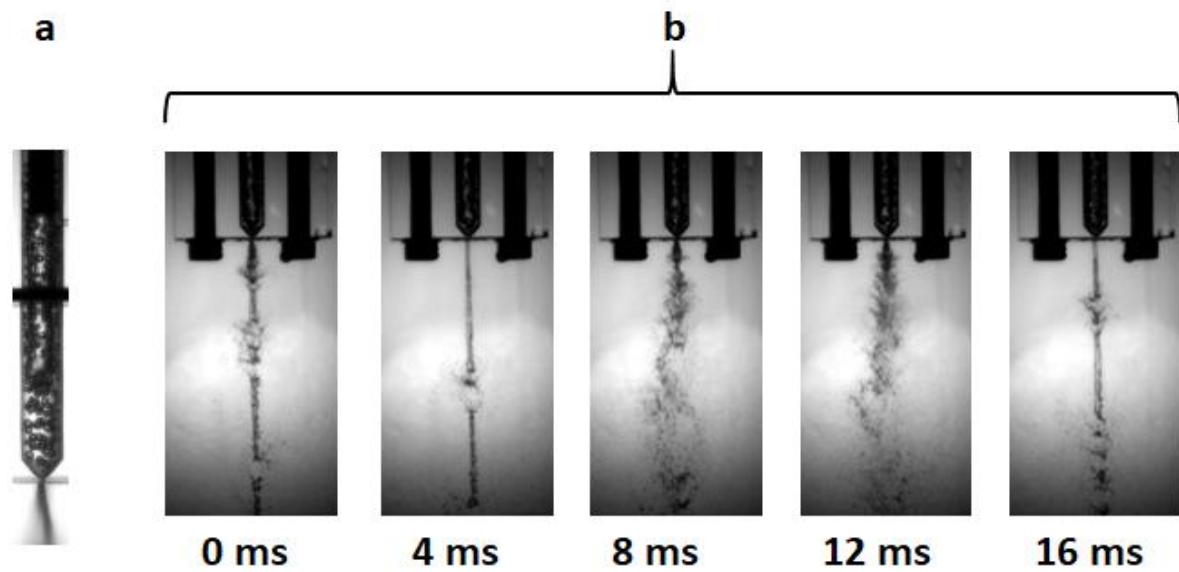


Figure 9. Atomisation of gas void disintegrated polydispersed bubbles (0.12% ALR):
a) internal flow, b) near-nozzle. Images are acquired by high-speed shadowgraphy.

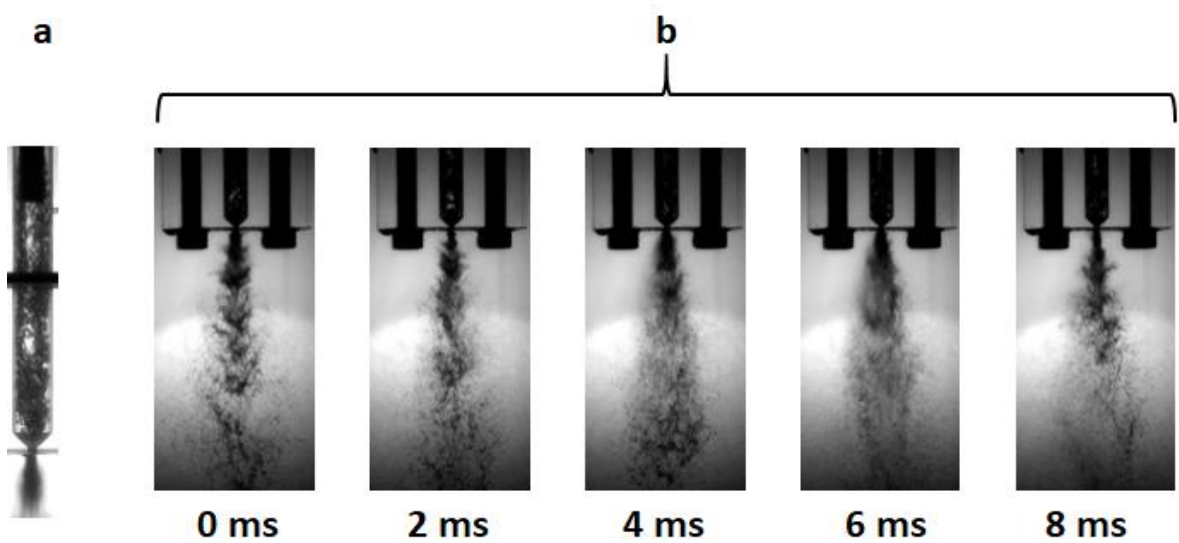


Figure 10. Atomisation of gas void disintegrated slug flow:
a) internal flow, b) near-nozzle. Images are acquired by high-speed shadowgraphy.

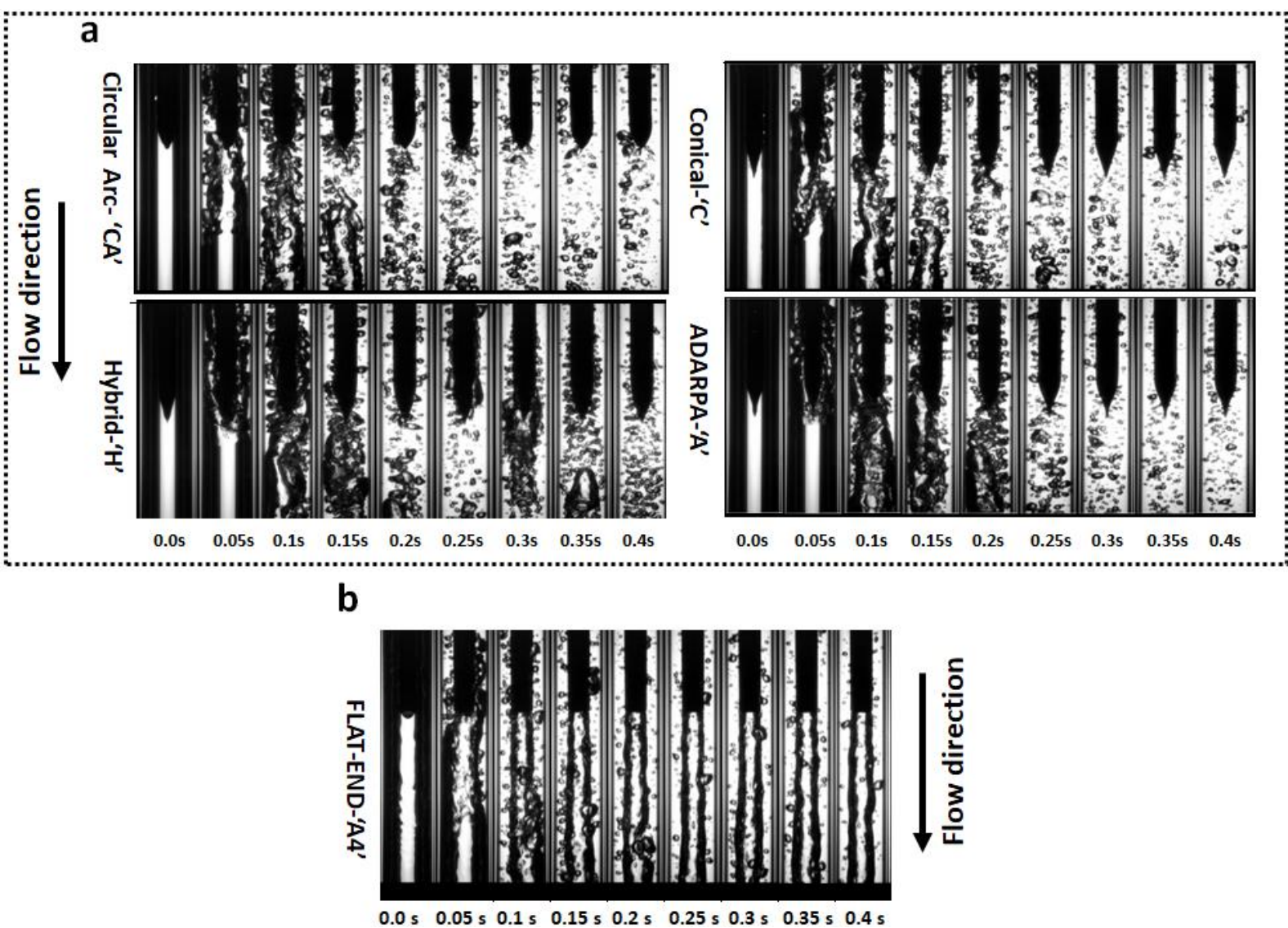


Figure 11. Ability of aerator tip to passively bleed mixing chamber of ambient gas: Liquid flow range: 75-289 g/s, 0% ALR; operating pressure: 5 bar.

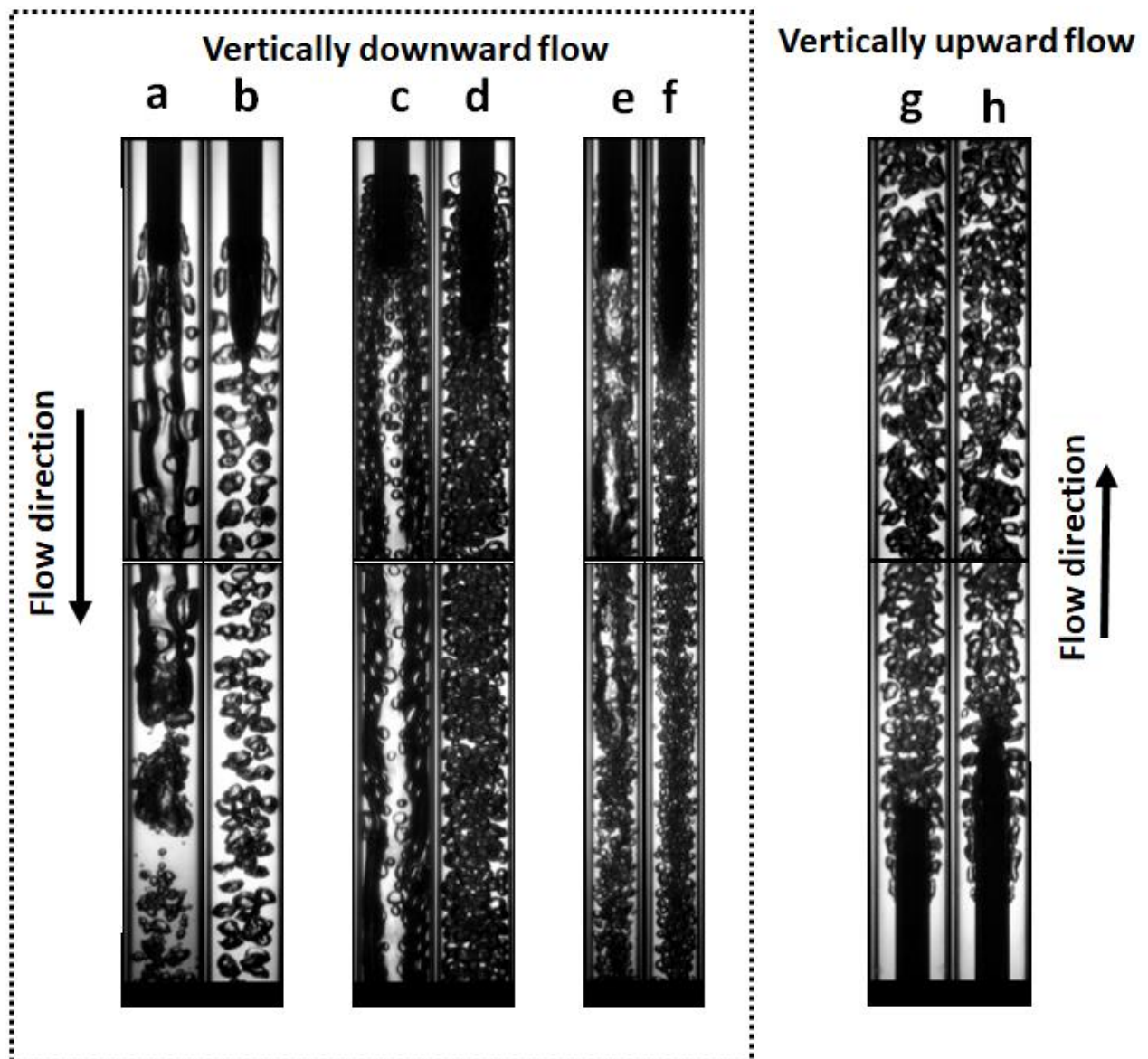


Figure 12. Comparison of flat-end and ADARPA aerator body designs for equivalent operating conditions: a) Flat-end: Liquid Baker parameter: $808.9 \text{ kg/m}^2\text{s}$, 0.13% ALR; b) ADARPA: Liquid Baker parameter: $802.5 \text{ kg/m}^2\text{s}$, 0.12% ALR; c) Flat-end: Liquid Baker parameter: $257.9 \text{ kg/m}^2\text{s}$, 0.26% ALR; d) ADARPA: Liquid Baker parameter: $261.1 \text{ kg/m}^2\text{s}$, 0.25% ALR; e) Flat-end: Liquid Baker parameter: $433.1 \text{ kg/m}^2\text{s}$, 0.25% ALR; f) ADARPA: Liquid Baker parameter: $433 \text{ kg/m}^2\text{s}$, 0.26% ALR; g) Flat-end: Liquid Baker parameter: $745 \text{ kg/m}^2\text{s}$, 0.25% ALR; h) ADARPA: Liquid Baker parameter: $748.4 \text{ kg/m}^2\text{s}$, 0.25% ALR.

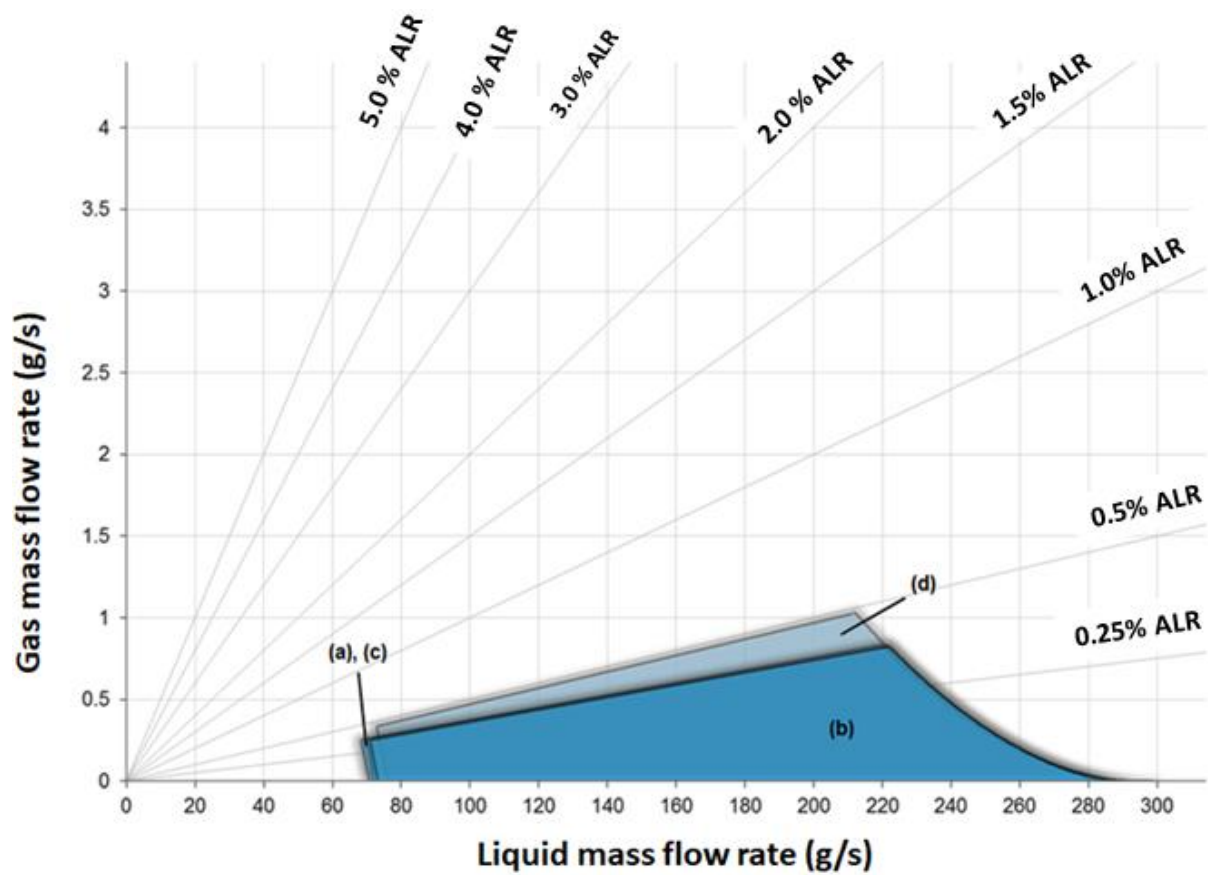


Figure 13. Effect of aerator body design on bubbly flow operating range: a) circular arc- 'CA' ; b) hybrid- 'H'; c) conical- 'C'; d) ADARPA- 'A'.

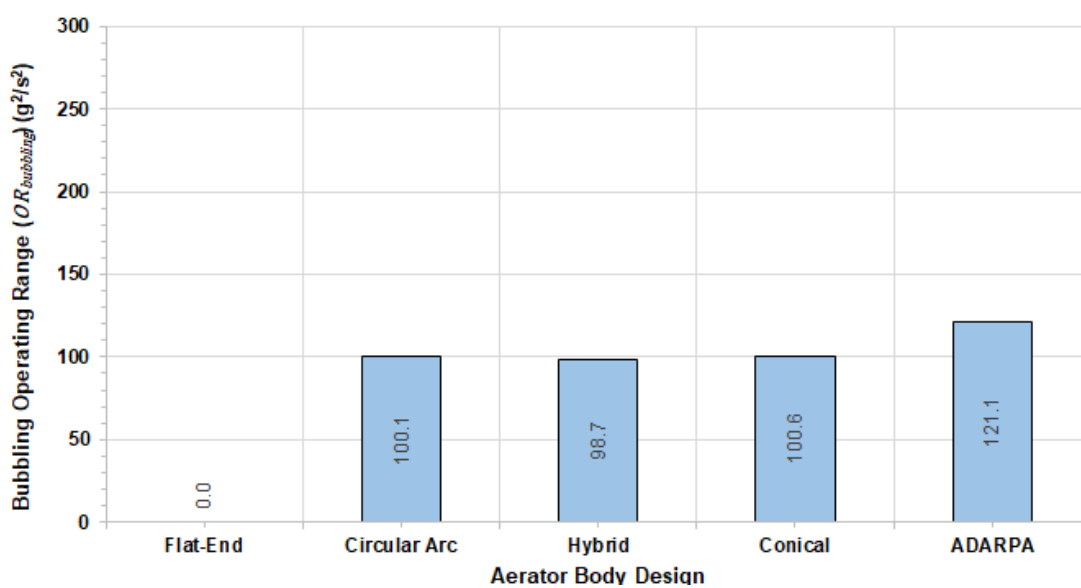


Figure 14. Effect of aerator body design on bubbly flow operating rang






	a)	b)	c)	d)	e)
					
	Circular Arc	Hybrid	Conical	ADARPA	Flat-end
Gas void:	Not cleared	Cleared	Cleared	Cleared	Not cleared
Conditions:	$G/\psi = 923 \text{ kg/m}^2$ $m_i = 289 \text{ g/s}$ $P = 5.0 \text{ barg}$	$G/\psi = 277 \text{ kg/m}^2$ $m_i = 87 \text{ g/s}$ $P = 0.4 \text{ barg}$	$G/\psi = 271 \text{ kg/m}^2$ $m_i = 85 \text{ g/s}$ $P = 0.4 \text{ barg}$	$G/\psi = 242 \text{ kg/m}^2$ $m_i = 76 \text{ g/s}$ $P = 0.3 \text{ barg}$	$G/\psi = 923 \text{ kg/m}^2$ $m_i = 289 \text{ g/s}$ $P = 5.0 \text{ barg}$

Figure 15. Ability of aerator tips to remove established gas void from wake

Experimental Parameter	Conventional flat-end aerator designs	Streamlined aerator designs
Discharge valve setting (g/s)	30-290	30-290
ALR (%)	0-5	0-5
Aerator Geometry	A1-A4	A4CA, A4C, A4H, A4A
Mixing chamber diameter (mm)	20	20
Operating pressure (bar)	5	5
Orientation	Vertically down and Vertically up	Vertically down

Table 1. Experimental test flow conditions employed for conventional flat-end and streamlined aerator body designs.